Crystal structure of the mixed conductor $Sr_4Fe_4Co_2O_{13}$

Helmer Fjellvåg,[a] Bjørn C. Hauback[b] and Rune Bredesen[c]

[a]*Department of Chemistry, University of Oslo, N-0315 Oslo, Norway*
[b]*Institutt for energiteknikk, N-2007 Kjeller, Norway*
[c]*SINTEF Materials Technology, P.O. Box 124 Blindern, N-0314 Oslo, Norway*

The crystal structure of $Sr_4Fe_4Co_2O_{13}$ has been determined on the basis of high-resolution powder neutron diffraction data. The space group is *Iba*2, $a=1103.19(16)$, $b=1898.63(26)$, $c=554.92(8)$ pm; $R(F^2)=0.117$, $R_{wp}=0.088$, $R_p=0.067$. In the investigated multi-phase sample, the $Sr_4Fe_4Co_2O_{13}$ phase exists as a major phase together with oxygen deficient $SrFeO_{3-x}$, in about equal mass fractions. $Sr_4Fe_4Co_2O_{13}$ is isostructural with $Sr_4Fe_6O_{13}$ and adopts a variant of the perovskite type-structure where layers of corner-sharing FeO_6 octahedra are separated by double layers of $(Fe,Co)O_4$ and $(Fe,Co)O_5$ coordination polyhedra. Condensed chains of $(Fe,Co)O_4$ and $(Fe,Co)O_5$ polyhedra run along [001]. Of the three non-equivalent Fe sites, the octahedral site is entirely occupied by Fe, the square pyramidal site by 61% Co and the trigonal pyramidal site by 52% Co. The refined chemical composition of the unit cell is $Sr_{16}Fe_{15.0}Co_{9.0}O_{51.84}$. Possible structural reasons for the reported very high ion conductivity of $Sr_4Fe_4Co_2O_{13}$ are discussed.

Mixed conducting oxides with high oxygen and electronic conduction are candidate materials for oxygen selective membranes. Recently, a new class of membrane materials, based on the Sr–Fe–Co–O system, has been reported with a very high oxygen conductivity in combination with a fairly high electronic conductivity.[1–3] The oxygen ion conductivity reported for $SrFeCo_{0.5}O_x$ at 800 °C of 7 S cm^{-1} is nearly an order of magnitude higher than reported for typical high oxygen conducting fluorite- and perovskite-type materials.[4–6] An explanation for the high oxygen-ion conductivity in this material, which has tentatively been described to have a layered perovskite type structure,[2] is not yet at hand. It seems reasonable to expect that such a high ionic conductivity should be reflected in the crystal structure properties of the material. The aim of present study is to throw light on the structural characteristics of the interesting $SrFeCo_{0.5}O_x$ material on the basis of powder X-ray and neutron diffraction data.

Experimental

Powder synthesis

Precursor materials of $Sr(NO_3)_2$, Fe_2O_3 and $Co(NO_3)_2\cdot 6H_2O$ were mixed in the ratio Sr : Fe : Co = 2 : 2 : 1 and milled with isopropyl alcohol for 3 h in a zirconia crucible. After milling and drying the powder mixture was calcined in air for 2 h at 800 °C or 950 °C, cooled to room temperature, and thereafter milled for 1 h in cyclohexane. Some samples were thereafter annealed at 800, 950 or 1200 °C. The sample used in the powder neutron diffraction study was in the last cycle heated for 14 h at 950 °C and 1 h at 1200 °C, before being finally cooled to room temperature.

Characterization

Powder X-ray diffraction data were collected with a Siemens D5000 diffractometer using Cu-Kα radiation and a flat plate sample holder, a secondary monochromator for the removal of fluorescence and a scintillation detector. The diffractogram for the nominal $SrFeCo_{0.5}O_x$ sample annealed at 1473 K corresponded to that published by Ma *et al.*[2] for their ion-conducting material. The powder samples were further studied in a scanning electron microscope (SEM) equipped with an energy dispersive spectrometer (EDS).

Powder neutron diffraction (PND) data were collected with the new PUS two-axis, high-resolution powder diffractometer[7] at the JEEP II reactor, Kjeller, Norway. Monochromatic neutrons, with wavelength $\lambda=153.8$ pm were obtained from Ge(511) at a take-off angle of around 90°. A cylindrical, vanadium sample holder of 5 mm diameter was used. Scattered data were collected by means of two banks of ^{3}He position-sensitive detectors (PSD). Each bank consists of an array of seven vertically displaced 600 mm PSD detectors covering 20° in 2θ. A complete diagram, from $2\theta=10$ to 130°, was obtained by moving the detector units in three steps. The collected data were converted to 2θ values in steps of $\Delta 2\theta=0.05°$ giving 2400 data points to be used in the Rietveld-type analysis.

Structure refinement

Least-squares profile refinements for the PND data were performed by means of the GSAS program.[8] The peak shapes were modelled by a Gaussian function. The background was simulated by means of a cosine Fourier series polynomial. Owing to a large number of atomic coordinate variables, soft distance restraints were introduced for the four, five and six coordinated iron/cobalt atoms during the refinements. The Fe/Co—O bond distances were restrained at 201.5 ± 2.0 (CN = 6), 194.8 ± 2.0 (CN = 5) and 186.5 ± 2.0 (CN = 4) pm on the basis of bond valence calculations[9] for bond orders 0.5, 0.6 and 0.75, respectively [selecting $R(Fe^{III}—O)=175.9$]. The diffraction pattern was found to reflect a multiphase sample (see Results). For each of the two major phases, $Sr_4Fe_4Co_2O_{13}$ and $SrFeO_{3-x}$, isotropic displacement factors were used, which were constrained to the same value for atoms of the same type (*i.e.*, for Sr, Fe/Co and O). The scattering amplitudes in the GSAS library, $b_{Sr}=7.02$, $b_{Fe}=9.54$, $b_{Co}=2.78$ and $b_O=5.81$ fm, were used. The atomic coordinates for the major additional phase, $SrFeO_{3-x}$, $0.0\leqslant x<0.5$, were initially not varied. In order to describe more correctly the non-stoichiometry in $SrFeO_{3-x}$, the occupation numbers for the subset of oxygen atoms giving either tetrahedral or octahedral coordination for the Fe/Co cations were refined. Altogether 38 coordinate parameters, 3 + 3 displacement factors, 4 + 2 occupation numbers, 3 + 3 unit-cell dimensions, 3 + 3 profile parameters, 12 background parameters, 1 scale factor, 1 phase fraction and 1 zero point were varied. In total, 79 free variables entered into the least-squares refinements. 822 Bragg reflections contributed to the observed profile consisting of 2400 data points.

Results and Discussion

The choice of annealing conditions has a strong effect on the observed powder X-ray diffraction pattern for samples with nominal composition $SrFeCo_{0.5}O_x$, *cf.* patterns for samples heat treated at 1073, 1223 and 1473 K in air in Fig. 1. The diagram for the sample annealed at 1473 K corresponds well to that published by Ma *et al.*[2] for a sample exhibiting remarkably high ion conductivity. The diffraction pattern for this sample has a striking similarity to the pattern[10] reported for $Sr_7Fe_{10}O_{22}$ in the JCPDS database. On the other hand, the pattern for the sample annealed at 1223 K has more similarities with those reported for $Sr_2Fe_2O_5$ and $SrFeO_3$.[11,12] It has been suggested that $Sr_7Fe_{10}O_{22}$ is identical to $Sr_4Fe_6O_{13}$ for which crystal structure data are available. Assuming this to be correct, the powder X-ray diffraction pattern was modelled by means of crystal structure data for $Sr_4Fe_6O_{13}$[13] and the Cerius[2] program system.[14] A quite good overall agreement was obtained. However, a few peaks remained unexplained. This indicated that additional phases were present in the sample. At this stage it appeared reasonable to rewrite the chemical formula as $Sr_4Fe_4Co_2O_{13}$, thereby indicating the structural relationship to $Sr_4Fe_6O_{13}$.

The powder X-ray diffraction pattern contained just a few reflections of reasonable intensity, clustered into groups throughout the pattern (see Fig. 1). No proper structure refinement of a large unit cell could be carried out with such sparse data. Therefore powder neutron diffraction data were collected with the high-resolution PUS diffractometer at Kjeller, Norway. In addition to facilitate proper determination of the positions of the light O atoms, the neutron diffraction data allowed the Fe and Co atoms to be distinguished, since their scattering amplitudes are substantially different (9.54 and 2.78 fm, respectively).

Examination of the peak profiles of the powder neutron diffraction pattern revealed the same non-explainable reflections as seen in the X-ray pattern. With support from scanning electron microscopy and EDS studies of different samples (see below), it became evident that the sample contained two major phases with somewhat different chemical compositions. In addition, SEM–EDS showed (very) small amounts of both Co- and Fe-rich phases, the latter possibly being $SrFe_{12}O_{19}$. Various binary and ternary oxides containing Sr, Fe and Co were evaluated on the basis of their diffraction patterns as possible additional phases. The non-explained reflections agreed well with non-stoichiometric strontium iron oxide, $SrFeO_{3-x}$ ($Sr_2Fe_2O_{5+\delta}$). The minority phases observed by SEM–EDS were neglected in the treatment of the diffraction data. Owing to the two- (multi-)phase nature of the sample, the complexity of the crystal structure description of the additional $SrFeO_{3-x}$ phase was kept to a minimum. Note that at least three distinct, closely related, phases exist for $SrFeO_{3-x}$, namely $SrFeO_3$ ($x=0.00$), $SrFeO_{2.75}$ ($x=0.25$) and $SrFeO_{2.50}$ ($x=0.50$; $Sr_2Fe_2O_5$), all with the possibility of Co replacing some of the Fe.

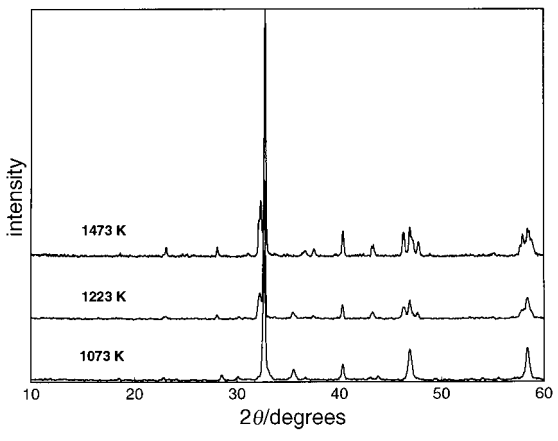

Fig. 1 Powder X-ray diffraction patterns (Cu-Kα radiation) of nominal $SrFeCo_{0.5}O_x$ samples, annealed at 1073, 1223 and 1473 K

Atomic coordinates for $Sr_4Fe_6O_{13}$ (space group *Iba*2)[13] and $Sr_2Fe_2O_5$ (space group *Ibm*2)[15,16] entered as starting point for the refinements, fixing z[Sr(2)] for $Sr_4Fe_4Co_2O_{13}$ and z[Fe(2)] [at (0, 0, z)] for $Sr_2Fe_2O_{5+\delta}$ to zero. After some refinement cycles a quite acceptable overall fit was obtained. However, the displacement factor for the oxygen atoms determining the tetrahedrally coordinated Fe atoms in $Sr_2Fe_2O_5$ was very high. Therefore, oxygen positions corresponding to an octahedral iron coordination, just like in $SrFeO_3$, were introduced. The refinement of the corresponding occupation numbers gave a rather oxidized strontium ferrite, $SrFeO_{2.84\pm0.05}$. The smaller unit-cell dimensions for the $SrFeO_{3-x}$ phase [$a=546.7(1)$, $b=1539.6(2)$, $c=547.6(1)$ pm; $V=460.9(1)\times10^6$ pm^3] relative to those reported for $Sr_2Fe_2O_5$ ($V=488.4\times10^6$ pm^3) correspond to a large amount of smaller Fe^{IV} atoms in the unit cell.

The refinements show that all atoms on the octahedral Fe(1) sites are iron, *cf.* Table 1. Cobalt is distributed over the five and four coordinated sites, Fe(2) and Fe(3), respectively. 61% of the atoms at the square-pyramidal Fe(2) site and 52% of the atoms at the trigonal-pyramidal Fe(3) site are cobalt. Note that Fe/Co is located in the basal plane of these pyramids. The refined amount of Co is somewhat higher than given by the assumed formula $Sr_4Fe_4Co_2O_{13}$, the refined unit-cell content being $Sr_{16}Fe_{14.98}Co_{9.02}O_{51.84}$. Judged from the PND data alone, the $SrFeO_{3-x}$ part of the sample contains no significant amount of cobalt. According to SEM–EDS results, most grains of $SrFeO_{3-x}$ appear to contain some cobalt. The content varied between different grains and was typically in the range $0.05<y<0.2$ for $SrFe_{1-y}Co_yO_{3-x}$ The refined phase fractions from PND are 52.9 mass% of $Sr_4Fe_4Co_2O_{13}$ and 47.1 mass% of $SrFeO_{3-x}$.

The PND result agrees well with the SEM observations of two major phases. One type consists of smooth rounded grains of approximately 3–10 μm in size, see Fig. 2. According to EDS these grains contain mainly Sr, Fe and O and are therefore assigned to the $SrFeO_{3-x}$ phase. The other type of grain, which constitutes the $Sr_4Fe_4Co_2O_{13}$ phase, has a plate-like or elongated crystallite shape. These grains were intimately mixed with the $SrFeO_{3-x}$ phase. The thickness of the $Sr_4Fe_4Co_2O_{13}$ grains was quite uniform, approximately 1–1.5 μm, whereas the other dimensions varied typically from 2 to 20 μm (for sample annealed at 1473 K).

From the Rietveld refinements the average cation composi-

Table 1 Crystal structure data[a] for $Sr_4Fe_4Co_2O_{13}$ derived from Rietveld-type refinement of powder neutron diffraction data (Kjeller, Norway) (calculated standard deviations in parentheses)

atom	x	y	z
Sr(1)	0.3855(29)	0.3376(11)	0.971(7)
Sr(2)	0.3716(29)	0.1560(11)	0.0000[b]
Fe(1)	0.1257(9)	0.2489(7)	0.983(7)
Fe(2)[c]	0.1124(14)	0.0380(9)	0.050(7)
Fe(3)[d]	0.1427(20)	0.4564(9)	0.012(6)
O(1)	0.1283(35)	0.1381(8)	0.961(9)
O(2)	0.1443(29)	0.3581(8)	0.973(6)
O(3)	0.0039(29)	0.2525(21)	0.241(8)
O(4)	0.2502(29)	0.2428(25)	0.234(8)
O(5)	0.2020(19)	0.0304(13)	0.360(7)
O(6)	0.3847(28)	0.0406(11)	0.850(6)
O(7)[e]	0.500000	0.500000	0.796(7)

[a]Space group *Iba*2, $a=1103.19(16)$, $b=1898.63(26)$, $c=554.92(8)$ pm. O(7) in 4a, all other atoms in 8c. Calculated density, ρ(X-ray)$=5.14$ g cm^{-3}. Isotropic displacement factors (in 10^4 pm^2) B(Sr)$=0.32(22)$, B(Fe/Co)$=0.56(19)$ and B(O)$=0.04(16)$. [b]Fixed. [c]Occupation number 0.57(4). [d]Occupation number 0.63(4). [e]Occupation number 0.96(4).

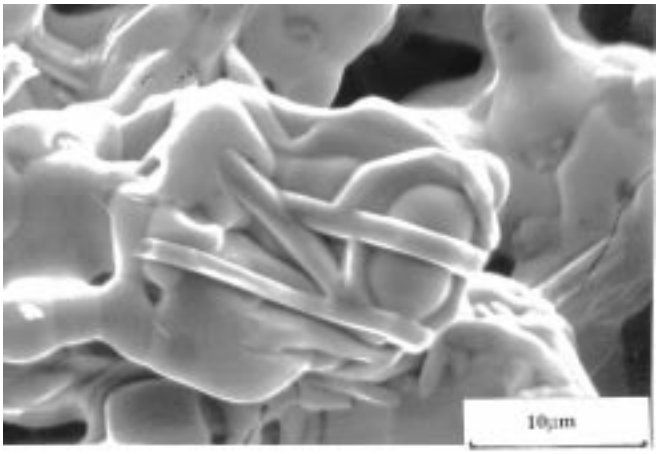

Fig. 2 SEM micrograph of $SrFeCo_{0.5}O_x$ powder heat-treated at 1200 °C

tion of the sample is calculated as $Sr_{1.00}Fe_{0.97}Co_{0.25}$ which, with respect to cobalt content, is considerably lower than nominally expected. This supports the finding by SEM–EDS of more phases actually being present in small amounts and that some of the $SrFeO_{3-x}$ phase may contain significant amounts of cobalt. However, the quality of the PND data with several overlapping reflections did not allow a more detailed analysis.

Refined atomic coordinates for $Sr_4Fe_4Co_2O_{13}$ are given in Table 1. Interatomic distances are listed in Table 2. The observed and difference powder neutron diffraction pattern is shown in Fig. 3. The reliability factors are $R(F^2)=0.117$, $R_p=0.067$, $R_{wp}=0.088$. The weak, rather broad Bragg reflections in Fig. 3, *e.g.* at $2\theta=19.5°$, are magnetic in origin, as proved by their large intensity enhancement on cooling, see the limited 2θ range in Fig. 4. The observed magnetic peaks (Fig. 4) resemble satellite reflections indicative of incommensurate magnetic order, possibly related to the helical spin structure reported for $SrFeO_3$.[17] Experiments on phase-pure material are required for determination of the magnetic structure.

The crystal structure of $Sr_4Fe_4Co_2O_{13}$ is schematically shown in Fig. 5. In the *ac* plane the unit cell of $Sr_4Fe_4Co_2O_{13}$ is related to the simple cubic perovskite-type unit cell by $a=2\sqrt{2}a_p$ and $c=\sqrt{2}a_p$. Perpendicular to [010], slabs of $(Fe,Co)_2O_3$ double layers enter between two-dimensional perovskite-type slabs of corner-sharing octahedra. An interesting question concerns the oxygen distribution in this transition metal double layer. In $Sr_4Fe_6O_{13}$ the O(7) site was reported

Table 2 Interatomic distances for $Sr_4Fe_4Co_2O_{13}$ in pm (calculated standard deviations in parentheses)

Sr(1)—O(1)	271(7)	Sr(2)—O(1)	272(6)
Sr(1)—O(1)	287(5)	Sr(2)—O(2)	294(5)
Sr(1)—O(1)	276(5)	Sr(2)—O(2)	302(5)
Sr(1)—O(2)	269(5)	Sr(2)—O(2)	264(5)
Sr(1)—O(3)	262(6)	Sr(2)—O(3)	263(6)
Sr(1)—O(3)	246(5)	Sr(2)—O(3)	264(4)
Sr(1)—O(4)	275(5)	Sr(2)—O(4)	249(5)
Sr(1)—O(4)	251(5)	Sr(2)—O(4)	277(5)
Sr(1)—O(5)	276(3)	Sr(2)—O(6)	236(3)
Fe(1)—O(1)	210.7(12)		
Fe(1)—O(2)	208.4(13)		
Fe(1)—O(3)	196.2(13)		
Fe(1)—O(3)	196.5(13)		
Fe(1)—O(4)	195.8(13)		
Fe(1)—O(4)	195.3(13)		
Fe(2)—O(1)	197.0(14)	Fe(3)—O(2)	187.9(14)
Fe(2)—O(5)	198.8(14)	Fe(3)—O(5)	192.5(13)
Fe(2)—O(5)	194.4(14)	Fe(3)—O(6)	185.7(14)
Fe(2)—O(7)	201.1(13)	Fe(3)—O(6)	190.3(13)
Fe(2)—O(7)	198.0(13)		

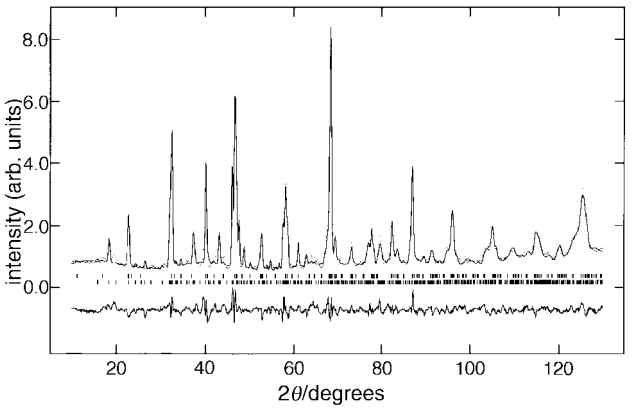

Fig. 3 Observed (dotted), calulated (full line) and difference (below) powder neutron diffraction pattern for $Sr_4Fe_4Co_2O_{13}$. $\lambda=153.8$ pm.

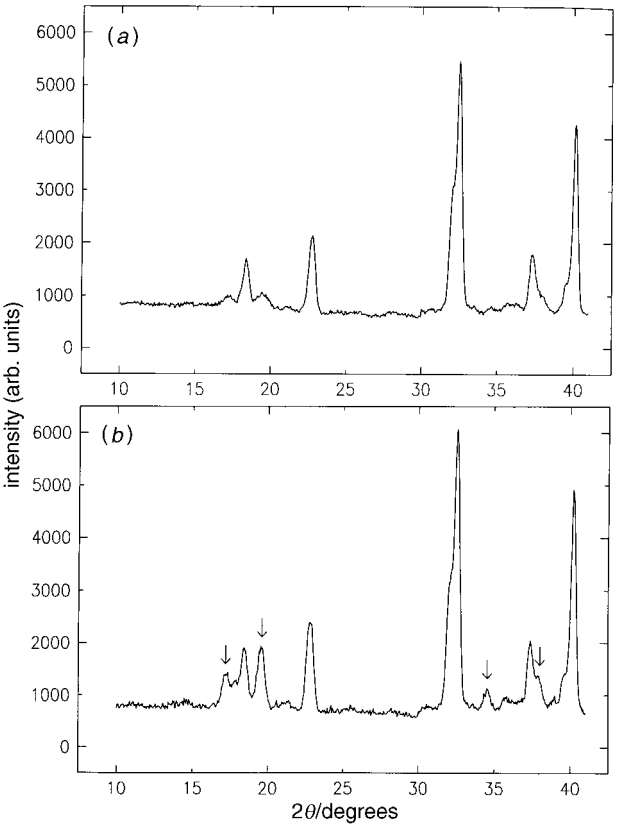

Fig. 4 Comparison of the low-angle parts of the powder neutron diffraction patterns at (*a*) 298 K and (*b*) 10 K. Arrows indicate reflections of magnetic origin.

to be completely filled.[13] However, one may envisage that oxygen atoms may also occupy an O(8) site, at around (0, 1/2, *ca.* 0.8), which will increase the coordination number for Fe(3) from four to five and provide trigonal-bipyramidal coordination. The present refinements can not, at a reasonable significance level, discriminate between models with varying degree of occupation of the O(7) and O(8) sites. Since the O(7) site increases the coordination from three- to five-fold for Fe(2), this site was, from crystal chemistry reasons, considered to be the one filled. This did not lead to a significant change in the reliability factors. The refined occupation number for O(7) is 0.96 ± 0.04. For a more complete description, experiments on phase-pure samples with different oxygen stoichiometries are required.

A comparison of the crystal structures of $Sr_4Fe_4Co_2O_{13}$, $Sr_2Fe_2O_5$ and $SrFeO_3$ is shown in Fig. 6. For slightly oxygen-

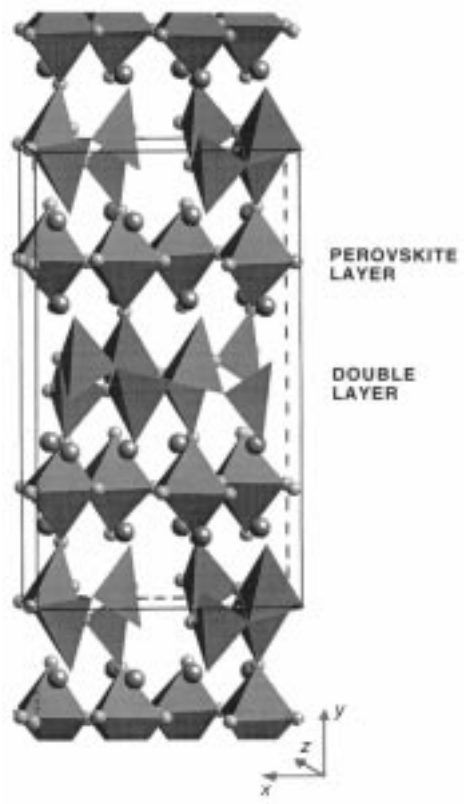

Fig. 5 Schematic drawing of the crystal structure of $Sr_4Fe_4Co_2O_{13}$

deficient $SrFeO_{3-x}$, $x \approx 0.0$, defect Fe octahedra (FeO_5 predominantly) are assumed to be randomly distributed throughout the structure. For $SrFeO_{2.5}$ ($=Sr_2Fe_2O_5$) the O vacancies are long-range ordered and layers containing chains of FeO_4 tetrahedra are formed between perovskite-type layers of corner-sharing octahedra. (Note that also another phase, $SrFeO_{2.75}$, with ordered oxygen vacancies has been reported.[16]) In $Sr_4Fe_4Co_2O_{13}$, the chains of tetrahedra in $Sr_2Fe_2O_5$ [see Fig. 7(*a*)] are replaced by a double layer of condensed trigonal and square pyramids [Fig. 7(*b*)]. All these Sr–Fe–(Co)–O phases contain layers of corner-sharing octahedra, and it appears probable that intergrowths may exist. The Sr–Fe–Co–O material may represent a semi-continuous series

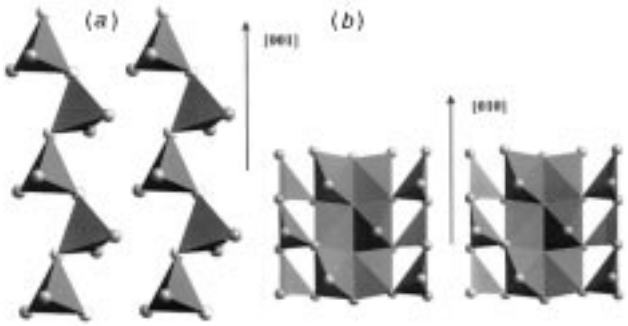

Fig. 7 Chains of corner-sharing tetrahedra in $Sr_2Fe_2O_5$ (*a*) and condensed chains of corner- and edge-sharing trigonal and square pyramids in $Sr_4Fe_4Co_2O_{13}$ (*b*)

of intergrowths where local order may easily be switched *via* oxygen atom movements.

The condensed chains in $Sr_4Fe_4Co_2O_{13}$ and the structural relationship to other oxygen-defect perovskite arrangements may provide a clue to understanding the ion conductivity of the material. In the transition metal double layer, the metal coordination seems flexible and may possibly vary between three and five during oxygen diffusion. Also in the octahedral layer the coordination is flexible with possibly local FeO_5 defect octahedra. The high oxygen diffusion may be related to the relatively large available volume per oxygen atom, the

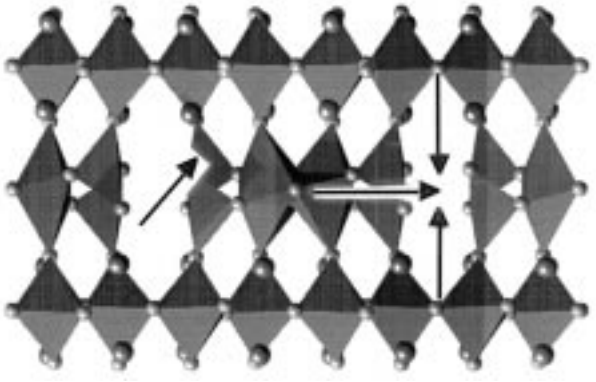

Fig. 8 Tentative schematic representation of possible oxygen movement in $Sr_4Fe_4Co_2O_{13}$

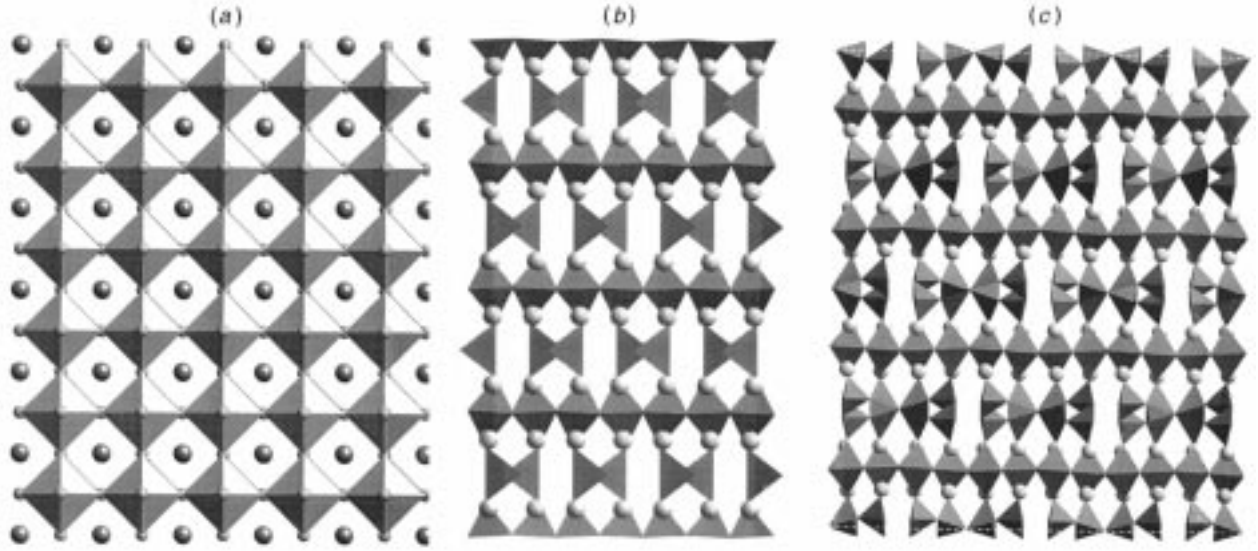

Fig. 6 Comparison of the perovskite-type related crystal structures of (*a*) $SrFeO_3$, (*b*) $Sr_2Fe_2O_5$ and (*c*) $Sr_4Fe_4Co_2O_{13}$ (drawn as ideally cubic)

flexible cation coordinations and possible three-dimensional diffusion paths with jumps on an atomic scale. [Simple estimates of the volume available to each oxygen in the structure, assuming cation spheres of Sr^{2+} ($r=113$ pm), Fe^{3+} ($r=64$ pm), $Co^{2+/3+}$ ($r=68$ pm), give (in 10^6 pm^3) $V=20.0$ for $Sr_4Fe_4Co_2O_{13}$, 21.6 for $Sr_2Fe_2O_5$ and 17.8 for $SrFeO_{2.84}$.] Several routes for jumps of oxygen atoms are possible within the double layer and to/from the perovskite-type layer. For instance, partial filling of the O(8) site or random vacancies in the O(7) site provide routes for one-dimensional oxygen conductivity, transport from the O(7) site to the O(8) site or *vice versa* may facilitate two-dimensional transport. Three-dimensionsal transport may be achieved when oxygen atoms jump out of the layer of octahedra into vacant O(7) or O(8) sites. Some possible routes for oxygen movement are tentatively drawn in Fig. 8.

References

1 U. Balachandran, J. T. Dusek, R. L. Mieville, R. B. Poeppel, M. S. Kleefisch, S. Pei, T. P. Kobylinski, C. A. Udovich and A. C. Bose, *Appl. Catal. A*, 1995, **133**, 19.
2 B. Ma, U. Balachandran, J.-H. Park and C. U. Segre, *Solid State Ionics*, 1996, **83**, 65.
3 B. Ma, U. Balachandran, J.-H. Park and C. U. Segre, *J. Electrochem. Soc.,* 1996, **143**, 1736.
4 H. Inaba and H. Tagawa, *Solid State Ionics*, 1996, **83**, 1.
5 T. Ishihara, H. Matsuda and Y. Takita, *J. Am. Chem. Soc.,* 1994, **116**, 3801.
6 B. C. H. Steele, *Mater. Sci. Eng. B,* 1992, **13**, 79.
7 B. C. Hauback, O. T. Buset, H. Fjellvåg, K. Johanson, J. Jørgensen and O. Steinsvoll, to be published.
8 A. L. Larson and R. B. von Dreele, *Program GSAS, General Structure Analysis System,* Los Alamos National Laboratories, Los Alamos, USA, 1994.
9 N. E. Brese and M. O'Keeffe, *Acta Crystallogr. Sect. B,* 1991, **47**, 192.
10 JCPDS, Powder Diffraction File, 22–1427.
11 JCPDS, Powder Diffraction File, 28–1227.
12 JCPDS, Powder Diffraction File, 39–0954.
13 A. Yoshiasa, K. Ueno, F. Kanamaru and H. Hiroyuki, *Mater. Res. Bull.*, 1986, **21**, 175.
14 Biosym/Molecular Simulations Inc., Cerius^2 — 2.0 program system, 1996.
15 M. Harder and H. Müller-Buschbaum, *Z. Anorg. Allg. Chem.*, 1980, **464**, 169.
16 C. Greaves, A. J. Jacobsen, B. C. Tofield and B. E. F. Fender, *Acta Crystallogr., Sect. B*, 1975, **31**, 641.
17 A. Oles, F. Kajzar, M. Kucab and W. Sikora, *Magnetic Structures Determined by Neutron Diffraction*, Panstwowe wydawnictwo naukowe, Warzawa, Krakow, 1976.

Paper 7/03727I; *Received* 29*th May*, 1997